

## Accepted Manuscript

CXCR7 contributes to the aggressive phenotype of cholangiocarcinoma cells

Alessandra Gentilini, Alessandra Caligiuri, Chiara Raggi, Krista Rombouts, Massimo Pinzani, Giulia Lori, Margherita Correnti, Pietro Invernizzi, Elisabetta Rovida, Nadia Navari, Sabina Di Matteo, Domenico Alvaro, Jesus M. Banales, Pedro Rodrigues, Carlotta Raschioni, Matteo Donadon, Luca Di Tommaso, Fabio Marra



PII: S0925-4439(19)30148-6  
DOI: <https://doi.org/10.1016/j.bbadis.2019.04.020>  
Reference: BBADIS 65464  
To appear in: *BBA - Molecular Basis of Disease*  
Received date: 23 February 2018  
Revised date: 20 December 2018  
Accepted date: 6 January 2019

Please cite this article as: A. Gentilini, A. Caligiuri, C. Raggi, et al., CXCR7 contributes to the aggressive phenotype of cholangiocarcinoma cells, *BBA - Molecular Basis of Disease*, <https://doi.org/10.1016/j.bbadis.2019.04.020>

This is a PDF file of an unedited manuscript that has been accepted for publication. As a service to our customers we are providing this early version of the manuscript. The manuscript will undergo copyediting, typesetting, and review of the resulting proof before it is published in its final form. Please note that during the production process errors may be discovered which could affect the content, and all legal disclaimers that apply to the journal pertain.

**CXCR7 contributes to the aggressive phenotype of cholangiocarcinoma cells**

Alessandra Gentilini<sup>1</sup>, Alessandra Caligiuri<sup>1</sup>, Chiara Raggi<sup>1,2</sup>, Krista Rombouts<sup>3</sup>, Massimo Pinzani<sup>3</sup>, Giulia Lori<sup>1</sup>, Margherita Correnti<sup>2</sup>, Pietro Invernizzi<sup>4</sup>, Elisabetta Rovida<sup>5</sup>, Nadia Navari<sup>1</sup>, Sabina Di Matteo<sup>6</sup>, Domenico Alvaro<sup>6</sup>, Jesus M. Banales<sup>7</sup>, Pedro Rodrigues<sup>7</sup>, Carlotta Raschioni<sup>8</sup>, Matteo Donadon<sup>9</sup>, Luca Di Tommaso<sup>10</sup>, and Fabio Marra<sup>1</sup>.

<sup>1</sup>Department of Experimental and Clinical Medicine, University of Florence, Italy, [alessandra.caligiuri@unifi.it](mailto:alessandra.caligiuri@unifi.it); [chiara.raggi@unifi.it](mailto:chiara.raggi@unifi.it); [giulia.lori@unifi.it](mailto:giulia.lori@unifi.it); [nadia.navari@unifi.it](mailto:nadia.navari@unifi.it); <sup>2</sup>Center for Autoimmune Liver Diseases IRCCS Istituto Clinico Humanitas, Rozzano (MI), Italy; [Margherita.Correntii@humanitasresearch.it](mailto:Margherita.Correntii@humanitasresearch.it); <sup>3</sup>University College London (UCL), Institute for Liver and Digestive Health, Royal Free Hospital, London, UK; [k.rombouts@ucl.ac.uk](mailto:k.rombouts@ucl.ac.uk); [m.pinzani@ucl.ac.uk](mailto:m.pinzani@ucl.ac.uk); <sup>4</sup>University of Milan Bicocca, Milan, Italy, [pietro.invernizzi@unimib.it](mailto:pietro.invernizzi@unimib.it); <sup>5</sup>Department of Experimental and Clinical Biomedical Sciences "Mario Serio", University of Florence, Italy; [elisabetta.rovida@unifi.it](mailto:elisabetta.rovida@unifi.it); <sup>6</sup>Department of Internal Medicine and Medical Specialties, Sapienza University of Rome, Rome, Italy; [sabina.dimatteo@uniroma1.it](mailto:sabina.dimatteo@uniroma1.it); [domenico.alvaro@uniroma1.it](mailto:domenico.alvaro@uniroma1.it); <sup>7</sup>Department of Liver and Gastrointestinal Diseases, Biodonostia Health Research Institute, CIBERehd, Ikerbasque, San Sebastian, Spain; [JESUS.BANALES@biodonostia.org](mailto:JESUS.BANALES@biodonostia.org); [PEDRO.RODRIGUES@biodonostia.org](mailto:PEDRO.RODRIGUES@biodonostia.org); <sup>8</sup>Oncology Experimental Therapeutics, Humanitas Clinical and Research Center, Rozzano, Milan, Italy; [carlotta.raschioni@humanitas.it](mailto:carlotta.raschioni@humanitas.it); <sup>9</sup>Department of Pathology, IRCCS Humanitas Clinical Institute, Rozzano, (MI), Italy; [matteo.donadon@humanitas.it](mailto:matteo.donadon@humanitas.it); <sup>10</sup>Pathology Unit, Humanitas Clinical and Research Center, Rozzano (MI), Italy and Department of Biomedical Sciences, Humanitas University, Rozzano (MI), Italy; [luca.di\\_tommaso@hunimed.eu](mailto:luca.di_tommaso@hunimed.eu).

**Corresponding Authors:**

Fabio Marra, MD, PhD  
Department of Experimental and Clinical Medicine  
University of Florence  
Largo Brambilla, 3  
I50134 Florence, ITALY  
Phone: +390557945425  
Fax: +390552758099  
E-mail: [fabio.marra@unifi.it](mailto:fabio.marra@unifi.it)

Or to :

Alessandra Gentilini, PhD  
Department of Experimental and Clinical Medicine  
University of Florence  
Largo Brambilla, 3  
I50134 Florence, ITALY  
Phone: +390552751801  
Fax: +390552758099  
E-mail: [alessandra.gentilini@unifi.it](mailto:alessandra.gentilini@unifi.it)

ACCEPTED MANUSCRIPT

**ABSTRACT**

Development of cholangiocarcinoma (CCA) is dependent on a cross-talk with stromal cells, which release different chemokines including CXCL12, that interacts with two different receptors, CXCR4 and CXCR7. The aim of the present study was to investigate the role of CXCR7 in CCA cells. CXCR7 is overexpressed by different CCA cell lines and in human CCA specimens. Knock-down of CXCR7 in HuCCT-1 cells reduced migration, invasion, and CXCL12-induced adhesion to collagen I. Survival of CCA was also reduced in CXCR7-silenced cells. The ability of CXCL12 to induce cell migration and survival was also blocked by CCX733, a CXCR7 antagonist. Similar effects of CXCR7 activation were observed in CCLP-1 cells and in primary iCCA cells. Enrichment of tumor stem-like cells by a 3D culture system resulted in increased CXCR7 expression compared to cells grown in monolayers, and genetic knockdown of CXCR7 robustly reduced sphere formation both in HuCCT-1 and in CCLP-1 cells. In HuCCT-1 cells CXCR7 was found to interact with  $\beta$ -arrestin 2, which was necessary to mediate CXCL12-induced migration, but not survival. In conclusion, CXCR7 is widely expressed in CCA, and contributes to the aggressive phenotype of CCA cells, inducing cell migration, invasion, adhesion, survival, growth and stem cell-like features. Cell migration induced by CXCR7 requires interaction with  $\beta$ -arrestin 2.

**Additional keywords:** Chemokines, liver stromal cells, cell migration, cancer stem cells,  $\beta$ -arrestin 2

**List of abbreviations:** AT, arsenic trioxide; H69, SV40-immortalized human cholangiocytes; MTT, 3-(4,5-dimethylthiazol-2-yl)-2,5-diphenyltetrazolium bromide; NT, non targeting; shRNA, short harping RNA; siRNA, small interfering RNA; NHC, human non-malignant cholangiocyte; HiBECS, Human intrahepatic biliary epithelial cells.

## 1. Introduction

Cholangiocarcinoma (CCA) is the second most common primary liver malignancy [1,2] but only limited information is available on its pathobiology, in spite of its poor prognosis and low response to current therapies [3,4]. CCA is characterized by the presence of neoplastic ductal structures surrounded by a considerable amount of fibrous stroma, comprised of myofibroblasts, small vessels and lymphoid cells. The presence of stromal tissue favors tumor progression and invasion of the normal hepatic parenchyma [5]. Secretion of several soluble mediators and expression of their cognate receptors has been shown to play a key role in tumor-stroma interactions [5,6]. Myofibroblasts derived from activated hepatic stellate cells (HSC) are the major contributors to collagen synthesis in chronic liver diseases [7], and have also been shown to promote CCA progression *in vitro* and *in vivo* [8], mostly through secretion of mediators which ultimately regulate the biology of CCA cells [5].

CXCL12 is a member of the CXC chemokine subfamily secreted by stromal fibroblasts, endothelial cells and, within the liver, HSC [9]. Studies in different types of tumor indicate that CXCL12 has a key role in promoting invasion and migration of cancer cells [10,11]. The G protein-coupled receptor, CXCR4 has been considered for many years the only receptor for CXCL12 [12]. Recent evidence indicates that CXCR7, another seven-transmembrane domain receptor, binds to CXCL12 with even higher affinity [13]. CXCR7 also binds to CXCL11, another chemokine family member [14].

Interestingly, CXCR7 may behave as a decoy (non-signaling) or signaling receptor depending on the cell type [12]. CXCR7 is expressed by many different tumor cells, and has been implicated in cell motility, adhesion, and angiogenesis [15,16]. Because CXCR7 expression has been associated with tumor aggressiveness, CXCR7 has been proposed as a prognostic marker in some types of cancer [17,18].

The molecular mechanisms of CCA progression are poorly understood, and this limits the development of effective therapies for this highly aggressive tumor. Here we show that CXCR7 is widely expressed in CCA, and its interaction with CXCL12 modulates the aggressive phenotype of CCA cells through intracellular signaling involving  $\beta$ -arrestin 2.

## 2. Material and methods

### 2.1 Materials

RPMI media was from Invitrogen (Carlsbad, CA, USA). Enhanced chemiluminescence (ECL) reagents and nitrocellulose membrane Hybond-C extra were from Amersham Pharmacia Biotech (Cologno Monzese, Milano, Italy), Immobilon Western reagents and ECM cell adhesion array kit were from Millipore Corporation (Billerica, MA, USA). Recombinant CXCL12 was purchased from R&D (Minneapolis, MN, USA). CCX733, CCX771 and CCX704 were kindly provided by Dr. Mark Penfold (Chemocentryx, Mountain View, CA, USA). Anti-CXCR7 antibody used for immunoprecipitation was from Biolegend (San Diego, CA, USA). Antibodies against CXCR4,  $\beta$ -arrestin 2, PARP and anti-CXCR7 antibodies used for Western blotting were from Abcam (Cambridge, United Kingdom). Immunohistochemistry was performed with an anti-CXCR7 Ab purchased from Proteintech (Rosemont, IL, USA). 3-(4,5-dimethylthiazol-2-yl)-2,5-diphenyltetrazolium bromide (MTT), arsenic trioxide (AT), monoclonal antibodies against  $\beta$ -actin and vinculin were purchased from Sigma (St. Louis, MO, USA). All other reagents were of analytical grade.

### 2.2 Cell culture

The CCA cell lines used in this study were kindly provided by Dr. A.J. Demetris, University of Pittsburgh (HuCCT-1, CCLP-1, SG231,) and Dr. G. Alpini, Temple, TX (MzCha1 and TFK1). The primary culture of normal human cholangiocyte, NHC, was provided By Dr.J.M.Banales [19]. HiBECs were purchased by ScienCell Research laboratories (Carlsbad, Germany).

Cells were cultured according to conditions described elsewhere [20]. Experiments were performed when cells reached about 90% confluence and after serum deprivation for 24 h.

### 2.3 Migration and invasion assays

Migration of HuCCT cells was assayed using modified Boyden chambers, essentially as described elsewhere [21,22]. Briefly, 20,000 cells were seeded in wells equipped with 8- $\mu$ m pore filters (Millipore Corp, MA, USA) and coated with rat tail collagen (20  $\mu$ g/ml) (Collaborative Biomedical Products, Bedford, USA) on the bottom side.

Chemoattractants were loaded in the lower chamber, while inhibitors, if present, were added to the upper chamber together with the cells. After 16 h incubation, cells

migrated to the underside of the filters were fixed, stained with Giemsa, mounted and counted at 40X magnification. All experiments were performed in duplicate. Each duplicate assay was repeated at least 3 times on separate occasions. Data are the average of cell counts obtained in 12 randomly chosen high-power fields (HPF). The procedure of the invasion assay was similar to the chemotaxis assay, but filters were coated on the top side with Matrigel (150 µg/ml) (BD Biosciences, MA, USA) and incubation was prolonged for 24 h.

#### *2.4 Cell survival*

The test was performed using MTT assay, as previously described [23]. 10000 cells/well were seeded in 96-well plates, incubated in complete medium for 24 h and serum-deprived for additional 24 h. Cells were then stimulated under different conditions. To measure cell viability, MTT solution (10 µl/well of a 5 mg/ml solution in PBS) was added to the cells the last hour of incubation time and the reaction was stopped by adding 20 µl of lysis solution (20% (w/v) SDS, 50% (v/v) N,N-dimethylformamide, 2% (v/v) acetic acid, 25 mM HCl, pH 4.7). Absorbance was read at 570 nm, in a Thermo Scientific Multiskan FC.

#### *2.5 Immunohistochemistry*

Twenty-three paraffin-embedded human liver tissue specimens were analyzed for the expression of CXCR7 by immunohistochemistry. All specimens were obtained after surgical resection and collected in the tissue bank of the Center for Autoimmune Liver Diseases, IRCCS Istituto Clinico Humanitas (Rozzano, Italy) after obtaining informed consent and approval of the local ethics committee. The investigated specimens included two samples of normal liver tissue and 21 specimens of CCA. Normal liver tissue was obtained from patients undergoing partial hepatectomy for a single colorectal cancer metastasis. In these cases, CXCR7 expression was evaluated in tissue distant at least 5 cm from the metastasis. All specimens of CCA were from previously untreated patients. Histology of the primary tumors was reviewed by pathologists experienced in liver tumors and classified according to the TNM staging system (Table 1).

For immunohistochemistry, paraffin sections were deparaffinized in xylene and rehydrated in graded ethanol to deionized water. Sections were then washed in 0.0005% PBS/Tween and subjected to endogenous peroxidase blocking with 3% H<sub>2</sub>O<sub>2</sub>, for 20 min at room temperature. Background Sniper buffer was used to block

unspecific binding (Biocare Medical, Concord CA). Immunostaining was performed with anti-CXCR7 antibodies (dilution 1:100). Sections were then washed in PBS-Tween and incubated with MACH1 Universal HRP-Polymer Detection kit (Biocare Medical, Concord CA) for 30 min at room temperature. The reaction was finally developed in Biocare's Betazoid DAB and counterstained with hematoxylin-eosin (DAKO, Glostrup, Denmark). The proportion of CXCR7-positive cell was classified into four grades (0,  $\leq 1\%$ ; 1, 1-30%; 2, 31-50%; 3, 51-100%). The staining intensity was graded from 0 to 3 (0, no staining; 1, weak staining; 2, moderate staining; 3, strong staining). The score in each section analyzed was obtained adding the two grades.

### *2.6 iCCA Primary Cell cultures*

The use of human materials and the research protocol were approved the Ethics Committees of the Policlinico Umberto I, University Hospital. Primary cell cultures were prepared, as previously described [24] [25] from specimens of human iCCA obtained from patients submitted to surgical resection. Primary cell cultures were maintained at 37°C in a humidified atmosphere of 5% CO<sub>2</sub> with H69 medium [24,25] and cultured for 3 passages before use.

### *2.7 RNA isolation and real time quantitative PCR*

Total RNA was isolated using the RNeasy kit (QIAGEN Sciences, MD) according to the manufacturer's recommendations, then 400 ng of RNA were examined by RTQ-PCR. FAM-labeled probes and primers for specific genes or for the housekeeping gene GAPDH were purchased from Applied Biosystems. Relative gene expression was calculated as  $2^{-\Delta Ct}$  ( $\Delta Ct = Ct$  of the target gene minus  $Ct$  of GAPDH) [11].

### *2.8 RNA interference transfection assay*

Transient gene silencing was performed by using human  $\beta$ -arrestin 2 validated siRNA and a non-specific-control siRNA (Custom SMARTpool siRNA Design Service of Dharmacon, Inc., Lafayette, CO). Transfection was performed using Lipofectamine RNAiMAX and Opti-MEM I reduced serum medium according to the manufacturer's instructions (Invitrogen). Western blot analysis was performed to confirm silencing. RNA interference was also performed by an Amaxa cell line Nucleofector kit L (Lonza, Basel, Switzerland) [26] using two shRNA plasmid constructs (10  $\mu$ g/10<sup>6</sup> cells) for human CXCR7 to obtain long term silencing. A control non-targeting (NT) shRNA plasmid construct expressing an shRNA sequence with no significant homology to any

mammalian transcript (Sigma Chemical Co. St. Louis, MO) was used as control (10  $\mu\text{g}/10^6$  cells). Treatment for 3 days with 0,5  $\mu\text{g}/\text{ml}$  of puromycin was performed to select the transfected cells.

### *2.9 Western blot analysis*

Cells were lysed at 4 °C with lysis buffer (1% Triton X-100, 50 mmol/L Tris-HCl, pH 7.4, 150 mmol/L NaCl, 1 mmol/L EDTA, 1 mmol/L sodium orthovanadate, 2 mmol/L PMSF, and 1 mmol/L each of leupeptin and pepstatin). After 30 min of lysis, cellular extracts were centrifuged 10 min at 12,000g, and the supernatant was used for Western blot experiments as detailed elsewhere [23].

### *2.10 Immunoprecipitation assay*

300  $\mu\text{g}$  of total protein were incubated with specific antibodies or control immunoglobulins at 4 °C for 2 h, as previously described [27]. Immune complexes were recovered by adding protein A-Sepharose beads (Amersham Pharmacia Biotech, Sweden) by overnight incubation with gentle shaking at 4°C. After washing three times in buffer (50 mM Tris-HCl, 0,5 mM NaCl, 1 mM  $\text{CaCl}_2$ , 1 mM  $\text{MgCl}_2$  and 0.1% Tween 20), the beads were analyzed by SDS-Page and Western blotting as described above [27].

### *2.11 Cell Adhesion Assay*

Adhesion assays were performed as described elsewhere [28]. Briefly, flat-bottom 96-well plates were coated with type I collagen (10  $\mu\text{g}/\text{mL}$ ) overnight at 4°C. Wells were then washed and incubated at 37°C for 2 h with heat-denatured bovine serum albumin to block nonspecific binding sites. Subsequently, 10000 cells/well (pretreated with 100 ng/ml CXCL12 when required) were seeded and incubated for 1 h at 37°C. Nonadherent cells were carefully removed by washing 3 times with DMEM. Adherent cells were fixed and stained with 0.5% crystal violet. Cell density was determined measuring the absorbance at 540 nm.

### *2.12 Cell proliferation assay*

Cell proliferation was performed using a colorimetric immunoassay based on the measurement of BrdU incorporation. 15000 cells/well were seeded in 96-well plates, incubated in complete medium for 24 hours and serum-starved for additional 24 hours.

The assay was performed following the manufacturer's protocol (Roche, Basel, Switzerland).

### 2.13 Sphere assay

Cells were grown in anchoring-independent conditions with selective serum-free DMEM/F12 medium supplemented with 1X B27 supplement minus vitamin A (Life Technologies), 20 ng/ml human recombinant epidermal growth factor, and 20 ng/ml bFGF (R&D System) for 15 days, as previously described [29]. To calculate sphere-forming efficiency, CCA cells were single-cell sorted into 96-well plates coated with an Ultra-Low Attachment Surface (Corning) using a FACS Aria (BD Biosciences). After 10 days, the amount of spheres formed was quantified, and expressed as the average number of formed sphere per microscopic field (20x) over five fields.

### 2.14 Cell growth assay

$10^4$  CCLP-1 cells were plated in 24-well dishes and incubated in medium deprived of serum for 24 hours. Cells were exposed to different stimuli and counted in triplicate at 36 hrs.

### 2.15 Human samples

iCCA samples from the San Sebastian (Spain) cohort were studied. All the samples were obtained from the Basque Biobank of the Donostia University Hospital. CXCR7 expression was measured by real-time qPCR. Research protocols were approved by the Clinical Research Ethics Committees of supporting institutions, and all patients signed written consents for the use of their samples for biomedical research. Total RNA was isolated from human liver samples (i.e. CCA tumors and surrounding liver tissue) using Tri-Reagent<sup>®</sup> (Sigma-Aldrich Co) following the manufacturer's instructions. Then, total RNA was reverse transcribed using the SuperScript Vilo cDNA Synthesis Kit (Invitrogen), according to manufacturer's instructions. qPCR was performed using the iQ<sup>™</sup> SYBR<sup>®</sup> Green Supermix (Bio-Rad) using the following primer sequences: CXCR7: 5'-CTAGAGGCTCCTTTCTGCAGTG-3' (forward) and 5'-GCAGATCCATCGTTCTGAGGC-3' (reverse); glyceraldehyde-3-phosphate dehydrogenase 5'-CCAAGGTCATCCATGACAAC-3' (forward) and 5'-TGTCATACCAGGAAATGAGC-3' (reverse). Gene expression was determined using the  $\Delta$ CT method and GAPDH was used as internal control for normalization of data. mRNA levels are represented as the percent increase over data obtained in normal surrounding liver tissue, set at 100.

### 2.16 Statistical analysis

Data in bar graphs represent mean $\pm$ SEM of at least three independent experiments. Statistical analysis was performed using Student's-t test. P values  $\leq 0.05$  were considered significant.

ACCEPTED MANUSCRIPT

### 3. Results

#### 3.1 CCA tissues and cell lines express CXCR7

We first analyzed CXCR7 immunoreactivity in 21 individual samples of CCA and in 2 samples of normal liver. The characteristics of the patients are reported in Table 1. In normal liver, CXCR7 expression was clearly detectable in bile ducts (Figure 1A). In all CCA specimens, a diffuse cytoplasmic staining for CXCR7 was clearly evident in tumor cells (Figure 1A) with the exception of two cases (Table 1). Notably, in the surrounding non-neoplastic tissue, bile ducts and endothelium retained remarkably high CXCR7 expression. We also compared CXCR7 gene expression in cultured normal human cholangiocytes (NHC), SV-40 immortalized H69 human cholangiocytes (non-malignant), and in human CCA cells, isolated from 4 patients with iCCA (Figure 1B). A marked and significant increase in *CXCR7* expression was evident in iCCA cells compared to non-tumor cells (Figure 1B). Expression of *CXCR4* tended to be higher in iCCA cells, although the results did not reach statistical significance due to the high variability of expression. Similarly,  *$\beta$ -arrestin 2* expression (Figure 1B) was higher in cells from patients with iCCA. In contrast, iCCA cells did not express detectable signal for *CXCL12*, as previously reported in HuCCT-1 cells [11].

We next evaluated whether different CCA cell lines express CXCR7. All intrahepatic (HuCCT-1, SG231, CCLP1) and extrahepatic (MzCha, TFK1) CCA cell lines tested were found to express CXCR7 (Figure 1C) at protein level. Of note, CXCR7 expression tended to be higher in all lines derived from intrahepatic CCA, in comparison to cells derived from extrahepatic tumors or HiBECs, an immortalized normal biliary epithelial cell line.

To establish a possible correlation between CXCR7 expression and tumor characteristics, gene expression was measured in samples obtained from patients with iCCA. In 15 patients expression levels in both tumor and surrounding non-tumoral tissue were available. Average CXCR7 expression was higher in iCCA, and the difference was borderline significant ( $100 \pm 28$  vs.  $356 \pm 151\%$ ,  $P=0.067$ ). Moreover, *CXCR7* expression tended to be higher in larger ( $> 50\text{mm}$ ) vs. smaller tumors, and in moderate/poorly differentiated vs. well-differentiated tumors (data not shown). However, these latter differences were not significant due to the low number of patients and the high variability in *CXCR7* gene expression. Similarly, we could not analyze the possible correlation with outcome.

### *3.2 CXCR7 inhibition contributes to CXCL12-induced adhesion, migration and invasiveness of HuCCT-1 cells*

We first evaluated the biologic characteristics relevant for the progression of CCA in HuCCT-1 cells, silencing CXCR7 with two specific shRNA (Figure 2A). CXCL12-mediated adhesion to culture wells coated with type I collagen was reduced in cells silenced for CXCR7 (Figure 2B). Moreover, CXCL12-induced chemo-invasion was also significantly reduced (Figure 2C). Because similar effects with both shRNAs, in the next set of experiments we decided to use only one shRNA specific for CXCR7. Experimental knockdown of CXCR7 expression resulted in reduced gene expression of MMP2 and MMP9, two metalloproteinases important for CCA invasiveness [30] and of VEGF (Figure 2D).

Silencing of CXCR7 significantly reduced CXCL12-elicited migration (Figure 3A). To provide additional support to this effect, we performed additional experiments using CCX733, a specific CXCR7 antagonist used in different tumors [31] [32] [33]. CCX733 prevented CXCL12-induced migration (Figure 3B), while CCX704, a compound structurally similar to CCX733 but inactive towards CXCR7, did not exert any significant actions (Figure 3C).

### *3.4 CXCR7 inhibition reduces survival of HuCCT-1 cells*

We next analyzed the effect of CXCR7 knock down on survival of HuCCT-1 cells. Increased survival induced by exposure to FBS (Figure 4A) was less evident when cells were silenced for CXCR7. Moreover, CXCR7 silencing prevented BrdU incorporation indicating a proliferative role of CXCR7 signaling (Figure 4E). In agreement with these results, in CXCR7-silenced cells cleaved PARP, an indicator of the apoptotic process, was more abundant than in control cells (Figure 4B), while total PARP decreased. These data indicate that CXCR7 contributes to mediate anti-apoptotic effects and to induce cell proliferation (Figure 4A, B and E). To further demonstrate the role of CXCR7 in mediating cell survival, we induced apoptosis exposing CCA cells to arsenic trioxide (AT). Decreased viability induced by this drug was reverted by co-incubation with CXCL12. In cells silenced for CXCR7 (Figure 4C) or exposed to the CXCR7 inhibitor, CCX733 (Figure 4D) the rescue induced by CXCL12 was no longer evident, indicating that CXCR7 activation is necessary to maintain cell survival.

### *3.5 CXCR7 inhibition contributes to CXCL12-induced migration, invasiveness, growth and survival of CCLP-1 cells*

To support the data obtained in HuCCT-1 cells, we performed additional experiments in CCLP-1, another iCCA line, using both genetic and pharmacological strategies to inhibit CXCR7 activity. Also in these cells, CXCL12-induced migration, invasion and growth (Figure 5), and these biologic actions were reduced after genetic knockdown of CXCR7 (Figure 5B, C, D). Of note, the ability of CXCL12 to rescue the pro-apoptotic effects of AT was blocked both by CXCR7 silencing or pretreatment with CCX 771, a specific CXCR7 antagonist (Figure 5E).

### *3.6 CXCR7 inhibition contributes to CXCL12-induced migration of primary iCCA cells*

To further expand the significance of these findings in the context of CCA, we conducted experiments in iCCA58 and iCCA60 cells, two primary cell lines derived as described in the Methods section. Both these cells expressed CXCR7 at levels comparable to those observed in HuCCT-1 (Figure 6A). In both types of cells, CXCL12 induced an increase in migration that was significantly reduced by preincubation with CCX711 (Figure 6B-C).

### *3.7 Role of CXCR7 in CXCL12-induced migration in hepatocarcinoma cells.*

Previous data indicate that CXCR7 is expressed by hepatocarcinoma (HCC) and HCC cells [34-36]. To establish whether regulation of the biology of liver tumor cells was unique to CCA, we conducted additional experiments in HuH7 and HepG2, two well-established HCC cells lines. Both lines expressed CXCR7 at the mRNA level (Supplementary Figure 1A). Moreover, activation of CXCR7 by CXCL12 induced cell migration, which was significantly reduced by preincubation with CCX733 or CCX771, two antagonist of CXCR7 (Supplementary Figure 1B-C).

### *3.8 3D cultures of CCA overexpress CXCR7*

We next analyzed the potential impact of CXCR7 activation in a 3D sphere system used as a functional tool to select for tumor stem-like cells. Spheres originated from HuCCT-1 cells had higher CXCR7 expression compared to parental cells grown in monolayer (Figure 5A). More importantly, genetic inhibition of CXCR7 robustly reduced sphere formation by HuCCT-1 and CCLP-1 cells (Figure 5B). These data indicate that CXCR7 expression is associated with the maintenance of a stemness-like status in CCA cells,

further supporting CXCR7 involvement in the aggressive phenotype of these cancer cells.

### *3.9 $\beta$ -arrestin 2 associates with CXCR7 and mediates CXCL12-induced migration*

$\beta$ -arrestin 2 has been shown to mediate the internalization and signaling of CXCR4 and CXCR7 in different cellular systems [31]. We examined the potential interaction between  $\beta$ -arrestin 2 and CXCR7 in HuCCT-1 cells. Immunoprecipitation of  $\beta$ -arrestin 2 followed by Western blotting for CXCR7 showed that these molecules are associated in baseline conditions, and this association is further increased upon CXCL12 treatment (Figure 6A). In addition, CXCR4, the other receptor for CXCL12, was shown to co-immunoprecipitate together with CXCR7, although no differences were found comparing unstimulated cells with cells exposed to CXCL12 (Figure 6B).

To investigate the functional role of  $\beta$ -arrestin 2 in CXCL12 signaling, HuCCT-1 cells were silenced using specific siRNA (Figure 6C). Knockdown of  $\beta$ -arrestin 2 significantly reduced the ability of CXCL12 to induce CCA cell migration (Figure 6D), while no changes were observed in the effects of CXCL12 on cell survival (Figure 6E). These data indicate that  $\beta$ -arrestin 2 participates in CXCR7 signaling in HuCCT-1 cells, but is not required for all biologic actions triggered by this receptor.

#### 4. Discussion

No effective therapies are available for surgically-untreatable CCA, and more detailed information on the biology of this tumor has the potential to identify novel therapeutic approaches, which represent a clear unmet need in oncology. CCA is characterized by an abundant stromal component, which modulates the biology of cancer cells through a complex intercellular cross-talk, also involving soluble mediators. Chemokines have been shown to regulate the aggressive phenotype of many types of cancer, including CCA [37], inducing a number of biologic actions via interaction with cognate receptors. In this study, we provide evidence for the first time that CXCR7, which binds the chemokine CXCL12, contributes to numerous and relevant phenotypic characteristics of CCA cells, potentially favoring cancer progression. Of note, CXCR7 was found to be present in many different CCA cell lines, where its abundance was higher than in a line of non-transformed biliary epithelial cells. CXCR7 gene expression was also more abundant in cells isolated from patients with iCCA than in non-tumor cholangiocytes. Expression of the *CXCR7* gene tended to be higher in tumor tissue than in the surrounding non-tumoral specimen, although statistical significance was only borderline due to wide dispersion of the data and the limited number of patients. Finally, CXCR7 immunostaining was present in 19/21 surgical samples of CCA, also in case with different levels of expression. The widespread expression of CXCR7 in cultured cells and in specimens collected from patients with CCA suggests a high biological relevance of this receptor. Moreover, while no data regarding CXCR7 expression in CCA have been previously reported, this receptor has been shown to mediate acquisition of an aggressive phenotype in many tumor cells and in activated tumor-associated endothelial cells [15,18,32,33,38].

In HuCCT-1 cells, a well-established cellular model of CCA, downregulation of CXCR7 by gene silencing reduced the ability of CXCL12 to increase migration, invasion of a basement-membrane like matrix, and adhesion to collagen-coated surfaces. In addition, CXCR7 was found to be involved in survival and proliferation of HuCCT-1 in response to CXCL12, both in the presence or absence of mitogenic factors. The ability of CXCR7 to modulate the biology of CCA was confirmed in another iCCA line, CCLP-1, and in two primary cells derived from patients with iCCA, demonstrating the general relevance of these findings. Of note, activation of CXCR7 was also found to regulate the migration of HCC cell lines. This latter observation is in agreement with previously reported data indicating widespread expression of CXCR7 in HCC cell lines, where activation of the receptor mediates proangiogenic signals, proliferation and invasion

[34-36]. Additionally, CXCR7 was found to be over-expressed in metastatic HCC and to correlate with a poor outcome [35]. Taken together, these lines of evidence suggest that the biological relevance of this receptor may be a general feature of hepatic cancer.

We found that gene expression of *MMP9* and *MMP2* was upregulated by the CXCL12/CXCR7 axis, similarly to what was observed in other types of cancer [35,39]. These effects are relevant in view of the fact that extracellular matrix (ECM) remodeling by matrix metalloproteinases (MMPs) [30] plays a relevant role in the biology of CCA, a cancer with high metastatic potential. Furthermore, gene expression of *VEGF*, that can modulate CCA cell migration [40] and induce angiogenesis, is increased by CXCL12 administration in a CXCR7-dependent fashion. Importantly, the critical role of CXCR7 in mediating these actions was confirmed with the use of a pharmacologic inhibitor of this receptor. This observation adds translational value to our findings, also considering that seven transmembrane, G-protein linked receptors may be good targets for drug development [41].

Until recently, the actions of CXCL12 were believed to be mediated by activation of CXCR4, which is also expressed on CCA cell lines where it regulates migration and survival [11]. More recently, CXCR7 has been unequivocally identified as an additional receptor mediating CXCL12's downstream signals [15]. Moreover, CXCR7 shows a 10-fold higher binding affinity for CXCL12 than CXCR4 [13]. Thus, it is possible that many of the actions elicited by CXCL12 in cancer cells and attributed uniquely to CXCR4 actually require the contribution of CXCR7. These observations may have an impact on the eventual development of therapeutic strategies involving this chemokine system. The combined involvement of CXCR7 and CXCR4 suggests that drugs targeting both receptors or interfering with ligand's binding could be more effective compared to blockade of a single receptor. Additional preclinical and clinical studies are required. We have also provided information on the signaling mechanisms activated by CXCR7 in CCA cells, and specifically on the role of  $\beta$ -arrestin 2. In other cells, CXCR7-mediated effects may be dependent or independent of  $\beta$ -arrestin 2 activation [42]. In HuCCT-1, CXCR7 and  $\beta$ -arrestin 2 were found to interact in a time- and ligand-dependent fashion. More important,  $\beta$ -arrestin 2 was necessary for CXCL12-induced chemotaxis, as previously reported in other cell types [43,44], but dispensable for CXCR7-mediated cell proliferation. As  $\beta$ -arrestin 2 may be itself a target for therapy, these lines of information may be helpful in understanding the fine tuning of signaling downstream the CXCL12/CXCR7 axis in this cancer cell type.

A very intriguing result of this study is related to the possible modulation of the cancer stem cell compartment by CXCR7. Cancer stem cells (CSCs) are critical for tumor initiation, progression and resistance to treatments, driving to recurrence after surgery and metastatic behavior[29] [45] . We used an in vitro model of anchorage-independent growth to enrich the CCA cell culture of stem-like cells, growing in spheroids. Expression of CXCR7 was higher in CCA stem-like cells, suggesting a role of CXCR7 in the acquisition of stemness features. More important, after CXCR7 knock-down, CCA cells were less able to form spheres, reinforcing the importance of this receptor in CCA aggressiveness. Further studies will be needed to identify the molecular mechanisms elicited by CXCR7 in CCA stem-like cells.

In conclusion, we have elucidated for the first time that CXCR7, highly expressed in CCA, plays a key role in the most important biological effects that lead to CCA aggressiveness. These results may contribute to identify potential new targets for cancer therapy, in consideration of the lack of effective therapies for CCA treatment.

**Conflicts of interest statement**

The authors have declared that no competing interest exists.

**FINANCIAL SUPPORT**

This work was financially supported by AIRC grant IG 2015 id. 17786 and by the University of Florence.

**ACKNOWLEDGEMENTS**

We thank AJ Demetris MD, of Department of Pathology, University of Pittsburgh, Pittsburgh, PA, for having provided us with the HuCCT-1 cells. We would also like to thank Dr. Mark Penfold from Chemocentryx (Mountain View, CA) for providing CCX733, CCX771 and CCX704. We are also grateful to Dr. Angela Provenzano, Department of Experimental and Clinical Medicine, University of Florence, Italy, for her contribution to HCC experiments. We are indebted to Darwish Shadya and Chiara Novello (Humanitas Clinical and Research Center) and Dr. Jesper Anderson (Anderson Group, Biotech Research and Innovation Centre, University of Copenhagen, Copenhagen, Denmark) for their help in CCA tissue preparation and analysis.

**FIGURE LEGENDS****Figure 1. CXCR7 expression in human liver tissue and CCA cells.**

**[A]:** expression of CXCR7 in normal human liver tissue (left panel) and CCA (right panel). In normal liver CXCR7 expression is present in bile ducts and blood vessels, while in CCA nearly all tumor cells express this receptor. **[B]:** Total RNA from normal human colangiocytes (NHC), the human immortalized cholangiocyte line H69, and CCA cells derived from 4 patients with intrahepatic CCA was analyzed for *CXCR7*, *CXCR4* and *β-arrestin 2* gene expression by RT-PCR. RNA expression is represented as fold-increase compared to control conditions. \* $P \leq 0.05$  vs. NHC, \*\* $P \leq 0.05$  vs. NHC and H69. In the *β-arrestin 2* panel, the CCA barogram represents the mean of 3 patients, with 'Δ' showing the value of an outlier **[C]:** cell lysates of different CCA lines were subjected to Western blot analysis for CXCR7. All lines were found to express CXCR7. Equal gel loading was assessed by actin blotting. Molecular weight markers are indicated on the right.

**Figure 2. CXCR7 is involved in CCA cell adhesion, invasion and expression of soluble mediators.**

**[A]:** HuCCT-1 cells were silenced for CXCR7 as reported in Materials and Methods, using two different shRNAs (shCXCR7-1 and shCXCR7-2) or with non-targeting (NT) shRNA (lane 1). Equal loading of the gel was assessed by the expression of vinculin (representative of  $n=3$ ). **[B, C]:** HuCCT-1 cells silenced for CXCR7 as described in [A] were incubated in the presence or absence of 100 ng/ml CXCL12, as indicated. Cell adhesion on type I collagen [B] and invasion of matrigel-coated filters [C] was assessed as indicated in Materials and Methods. The number of cells migrated is represented as fold-increase compared to control conditions. \* $P \leq 0.05$  vs. control, \*\* $P \leq 0.05$  vs. shNT ( $n=3$ ). **[D]:** Total RNA from cells silenced for CXCR7 (shCXCR7-2) incubated in the presence or absence of CXCL12 for 8 hours (left and middle panels) or 24 hours (right panel) was analyzed for expression of *MMP2*, *MMP9*, and *VEGF* by RT-PCR. RNA expression is represented as fold-increase compared to control conditions. \* $P \leq 0.05$  vs. unstimulated control, \*\* $P \leq 0.05$  vs. shNT ( $n=3$ ).

**Figure 3. Genetic knockdown or pharmacological antagonism of CXCR7 blocks CXCL12-induced migration.**

**[A]** HuCCT-1 cells were silenced for CXCR7 or with non-targeting (NT) shRNA, and incubated in the presence or absence of 100 ng/ml CXCL12, as indicated. Cell

migration was measured as indicated in Materials and Methods. The number of cells migrated is represented as fold-increase compared to control conditions. \* $P \leq 0.05$  vs. unstimulated control;  $\Delta P \leq 0.05$  vs. shNT (n=3). **[B]**: HuCCT-1 cells were incubated in the presence or absence of 100 ng/ml CXCL12, with or without a 30 min pretreatment with different concentrations of the CXCR7 antagonist, CCX733, and cell migration was measured. \* $P \leq 0.05$  vs unstimulated control; \*\* $P \leq 0.05$  vs. CXCL12 (n=3). **[C]**: The experiment was performed as described in panel [B], using CCX704, an inactive compound structurally similar to CCX733. \* $P \leq 0.05$  vs. unstimulated control (n=3).

**Figure 4. Genetic knockdown or pharmacological antagonism of CXCR7 reduces CCA survival and proliferation.**

**[A]**: HuCCT-1 cells were silenced for CXCR7 or with non-targeting (NT) shRNA, and incubated in the presence or absence of different concentrations of FBS, as indicated. Cell survival was evaluated at time 0 and after 48 hours, and is represented as fold-increase compared to control conditions. \* $P \leq 0.05$  vs. unstimulated control at 48 hours;  $\Delta P \leq 0.05$  vs. shNT (n=3). **[B]**: HuCCT-1 cells were silenced for CXCR7 or with non-targeting (NT) shRNA, and incubated in the presence or absence of different concentrations of FBS, as indicated, for 24 hours. Western blot analysis with an antibody recognizing both total PARP and cleaved PARP was performed as indicated in Materials and Methods. Equal loading of the gel was assessed by GAPDH expression. Densitometry measured in four different experiments is shown in the lower panel. \* $P \leq 0.05$  versus shNT. **[C]** HuCCT-1 cells were silenced for CXCR7 or with non-targeting (NT) shRNA, in the presence or absence of 0.05 mM arsenic trioxide (AT) and/or 100 ng/ml CXCL12, as indicated. Cell survival was measured by MTT assay. \* $P \leq 0.05$  vs. unstimulated control; \*\* $P \leq 0.05$  vs. AT alone (n=3). **[D]** HuCCT-1 cells were incubated in the presence or absence of 0.05 mM arsenic trioxide (AT), with or without a 30 min pretreatment with 100nM CCX733, and cell survival was measured by MTT assay. \* $P \leq 0.05$  vs. unstimulated control; \*\* $P \leq 0.05$  vs. AT alone (n=3)  $\Delta P \leq 0.05$  vs. AT+CXCL12. **[E]** HuCCT-1 cells were silenced for CXCR7 or with non-targeting (NT) shRNA, and incubated in the presence or absence of 10% FBS, as indicated, for 24 hours. Cell proliferation was assessed by BrdU incorporation. Cells BrdU incorporation is represented as fold-increase compared to control conditions. \* $P \leq 0.05$  vs. unstimulated control; \*\* $P \leq 0.05$  vs. shNT (n=3).

**Figure 5. Genetic knockdown of CXCR7 reduces CCA migration, invasion, growth and survival of CCLP-1 cells.**

**[A]:** CCLP-1 cells were silenced for CXCR7 or with non-targeting (NT) shRNA and CXCR7 expression was measured by Western blotting as described in Materials and Methods. as indicated. Equal loading of the gel was assessed by the expression of vinculin (representative of n=3). **[B, C]:** CCLP-1 cells were silenced for CXCR7 or with non-targeting (NT) shRNA, and incubated in the presence or absence of 100 ng/ml CXCL12, as indicated. Cell invasion and migration were measured as indicated in Materials and Methods. The number of cells migrated is represented as fold-increase compared to control conditions. \* $P \leq 0.05$  vs. unstimulated control; \*\*  $P \leq 0.05$  vs. shNT (n=3). **[D]:** CCLP-1 cells were silenced for CXCR7 or with non-targeting (NT) shRNA and incubated in the presence or absence of 1% or 10% FBS, as indicated. Cell count was measured after 36 hrs of incubation. \* $P \leq 0.05$  vs. unstimulated control;  $\Delta P \leq 0.05$  vs. shNT (n=3). **[E]:** CCLP-1 cells were silenced for CXCR7 or with non-targeting (NT) shRNA, and incubated in the presence or absence of 0.05  $\mu\text{M}$  arsenic trioxide (AT) and/or 100 ng/ml CXCL12, as indicated. shNT cells were also incubated in the presence or absence of AT and with or without a 30 min pretreatment with 100nM CCX771, a specific CXCR7 antagonist. Cell survival was measured by MTT assay. \* $P \leq 0.05$  vs. unstimulated control;  $\Delta P \leq 0.05$  vs. AT alone; \*\* $P \leq 0.05$  vs. AT+CXCL12 (n=3).

**Figure 6. Pharmacological antagonism of CXCR7 blocks CXCL12-induced migration of primary iCCA cells.**

**[A]:** Primary cell lines derived from two different patients affected by iCCA (iCCA58 and iCCA60) were analyzed for CXCR7 expression in comparison to HuCCT-1 (positive control). Equal loading of the gel was assessed by the expression of vinculin. **[B, C]:** iCCA58 and iCCA60 were incubated in the presence or absence of 100 ng/ml CXCL12, with or without a 30 min pretreatment with the CXCR7 antagonist CCX771 (100 nM). Cell migration was measured as described in Materials and Methods. \* $P \leq 0.05$  vs unstimulated control; \*\* $P \leq 0.05$  vs. CXCL12 (n=3).

**Figure 7. CXCR7 expression contributes to the acquisition of stem cell-like features in HuCCT-1 cells.**

**[A]:** Cell lysates from HuCCT-1 cells cultured in monolayer or after sphere formation were analyzed for CXCR7 expression using Western blot analysis. Equal loading was assessed by the expression of vinculin. Densitometry values of three different

experiments is indicated below. \*  $P \leq 0.05$  vs. monolayer. **[B]**: HuCCT-1 or CCLP-1 cells were silenced for CXCR7 or with non-targeting (NT) shRNA and the number of spheres formed was measured as described in Materials and Methods. Each experiment was performed in triplicate. Mean  $\pm$  SD of 4 independent experiments, \*  $P \leq 0.05$  versus shNT.

**Figure 8. Interaction between CXCR7 and  $\beta$ -arrestin 2 mediates CCA cell migration but not survival.**

**[A]**: HuCCT-1 cells were incubated with 100 ng/ml CXCL12 for different periods of time, as indicated. Cell lysates were immunoprecipitated with an antibody against  $\beta$ -arrestin 2 and used for Western blot analysis under non-reducing conditions to detect CXCR7 or  $\beta$ -arrestin 2. **[B]**: (Upper panel) HuCCT-1 cells were incubated with 100 ng/ml of CXCL12 for 10 minutes, and cell lysates were immunoprecipitated with an antibody against CXCR7 and used for Western blot analysis under non-reducing conditions to detect CXCR4 (Lower panel). Western blot for CXCR4 was conducted with cell lysates collected before and after the immunoprecipitation as control of the IP experiment (representative of  $n=3$ ). **[C]**: HuCCT-1 cells were silenced for  $\beta$ -arrestin 2 as indicated in Materials and Methods, or with scrambled (SC) siRNA. Equal loading of the gel was assessed by the expression of vinculin (representative of  $n=3$ ). **[D]**: HuCCT-1 cells silenced for  $\beta$ -arrestin 2 as described in **[C]** were incubated in the presence or absence of 100ng/ml CXCL12, as indicated, and cell migration was measured. The number of cells migrated is represented as fold-increase compared to control conditions. \* $P \leq 0.05$  vs. unstimulated control;  $\Delta P \leq 0.05$  vs. siSC cells treated with CXCL12 ( $n=3$ ). **[E]** The experiment was performed as in **[D]**, and cell survival was measured by MTT assay in cells exposed to 0.05  $\mu$ M arsenic trioxide (AT) in the presence or absence of 100ng/ml CXCL12. Cell survival is represented as fold-increase compared to control conditions. \* $P \leq 0.05$  vs. unstimulated control; \*\* $P \leq 0.05$  vs. AT alone ( $n=3$ ).

**REFERENCES**

- [1] Zhao DY, Lim KH. Current biologics for treatment of biliary tract cancers. *J Gastrointest Oncol* 2017;8:430-40.
- [2] Rizvi S, Gores GJ. Pathogenesis, diagnosis, and management of cholangiocarcinoma. *Gastroenterology* 2013;145:1215-29.
- [3] Briggs CD, Neal CP, Mann CD, Steward WP, Manson MM, Berry DP. Prognostic molecular markers in cholangiocarcinoma: a systematic review. *Eur J Cancer* 2009;45:33-47.
- [4] Kayhanian H, Smyth EC, Braconi C. Emerging molecular targets and therapy for cholangiocarcinoma. *World J Gastrointest Oncol* 2017;9:268-80.
- [5] Cadamuro M, Stecca T, Brivio S, Mariotti V, Fiorotto R, Spirli C, et al. The deleterious interplay between tumor epithelia and stroma in cholangiocarcinoma. *Biochim Biophys Acta* 2017.
- [6] Ohira S, Sasaki M, Harada K, Sato Y, Zen Y, Isse K, et al. Possible regulation of migration of intrahepatic cholangiocarcinoma cells by interaction of CXCR4 expressed in carcinoma cells with tumor necrosis factor-alpha and stromal-derived factor-1 released in stroma. *Am J Pathol* 2006;168:1155-68.
- [7] Friedman SL. Hepatic stellate cells: protean, multifunctional, and enigmatic cells of the liver. *Physiol Rev* 2008;88:125-72.
- [8] Okabe H, Beppu T, Hayashi H, Ishiko T, Masuda T, Otao R, et al. Hepatic stellate cells accelerate the malignant behavior of cholangiocarcinoma cells. *Ann Surg Oncol* 2011;18:1175-84.
- [9] Sawitza I, Kordes C, Reister S, Haussinger D. The niche of stellate cells within rat liver. *Hepatology* 2009;50:1617-24.
- [10] Matsusue R, Kubo H, Hisamori S, Okoshi K, Takagi H, Hida K, et al. Hepatic stellate cells promote liver metastasis of colon cancer cells by the action of SDF-1/CXCR4 axis. *Ann Surg Oncol* 2009;16:2645-53.
- [11] Gentilini A, Rombouts K, Galastri S, Caligiuri A, Mingarelli E, Mello T, et al. Role of the stromal-derived factor-1 (SDF-1)-CXCR4 axis in the interaction between hepatic stellate cells and cholangiocarcinoma. *Journal of Hepatology* 2012;57:813-20.
- [12] Sun X, Cheng G, Hao M, Zheng J, Zhou X, Zhang J, et al. CXCL12 / CXCR4 / CXCR7 chemokine axis and cancer progression. *Cancer Metastasis Rev* 2010;29:709-22.
- [13] Luker KE, Gupta M, Steele JM, Foerster BR, Luker GD. Imaging ligand-dependent activation of CXCR7. *Neoplasia* 2009;11:1022-35.

- [14] Benredjem B, Girard M, Rhainds D, St-Onge G, Heveker N. Mutational Analysis of Atypical Chemokine Receptor 3 (ACKR3/CXCR7) Interaction with Its Chemokine Ligands CXCL11 and CXCL12. *J Biol Chem* 2017;292:31-42.
- [15] Burns JM, Summers BC, Wang Y, Melikian A, Berahovich R, Miao Z, et al. A novel chemokine receptor for SDF-1 and I-TAC involved in cell survival, cell adhesion, and tumor development. *J Exp Med* 2006;203:2201-13.
- [16] Zhao ZW, Fan XX, Song JJ, Xu M, Chen MJ, Tu JF, et al. ShRNA knock-down of CXCR7 inhibits tumour invasion and metastasis in hepatocellular carcinoma after transcatheter arterial chemoembolization. *J Cell Mol Med* 2017.
- [17] Schrevel M, Karim R, ter Haar NT, van der Burg SH, Trimbos JB, Fleuren GJ, et al. CXCR7 expression is associated with disease-free and disease-specific survival in cervical cancer patients. *Br J Cancer* 2012;106:1520-5.
- [18] Guo JC, Li J, Zhou L, Yang JY, Zhang ZG, Liang ZY, et al. CXCL12-CXCR7 axis contributes to the invasive phenotype of pancreatic cancer. *Oncotarget* 2016;7:62006-18.
- [19] Banales JM, Cardinale V, Carpino G, Marzioni M, Andersen JB, Invernizzi P, et al. Expert consensus document: Cholangiocarcinoma: current knowledge and future perspectives consensus statement from the European Network for the Study of Cholangiocarcinoma (ENS-CCA). *Nat Rev Gastroenterol Hepatol* 2016;13:261-80.
- [20] Han C, Demetris AJ, Michalopoulos GK, Zhan Q, Shelhamer JH, Wu T. PPARgamma ligands inhibit cholangiocarcinoma cell growth through p53-dependent GADD45 and p21 pathway. *Hepatology* 2003;38:167-77.
- [21] Novo E, Cannito S, Zamara E, Valfre di Bonzo L, Caligiuri A, Cravanzola C, et al. Proangiogenic cytokines as hypoxia-dependent factors stimulating migration of human hepatic stellate cells. *Am J Pathol* 2007;170:1942-53.
- [22] Bonacchi A, Romagnani P, Romanelli RG, Efsen E, Annunziato F, Lasagni L, et al. Signal transduction by the chemokine receptor CXCR3: activation of Ras/ERK, Src, and phosphatidylinositol 3-kinase/Akt controls cell migration and proliferation in human vascular pericytes. *J Biol Chem* 2001;276:9945-54.
- [23] Rovida E, Di Maira G, Tusa I, Cannito S, Paternostro C, Navari N, et al. The mitogen-activated protein kinase ERK5 regulates the development and growth of hepatocellular carcinoma. *Gut* 2015;64:1454-U160.
- [24] Fraveto A, Cardinale V, Bragazzi MC, Giuliente F, De Rose AM, Grazi GL, et al. Sensitivity of Human Intrahepatic Cholangiocarcinoma Subtypes to Chemotherapeutics

- and Molecular Targeted Agents: A Study on Primary Cell Cultures. *PLoS One* 2015;10:e0142124.
- [25] Lustri AM, Di Matteo S, Fraveto A, Costantini D, Cantafora A, Napoletano C, et al. TGF-beta signaling is an effective target to impair survival and induce apoptosis of human cholangiocarcinoma cells: A study on human primary cell cultures. *PLoS One* 2017;12:e0183932.
- [26] Petta S, Valenti L, Marra F, Grimaudo S, Tripodo C, Bugianesi E, et al. MERTK rs4374383 polymorphism affects the severity of fibrosis in non-alcoholic fatty liver disease. *J Hepatol* 2016;64:682-90.
- [27] Rombouts K, Lottini B, Caligiuri A, Liotta F, Mello T, Carloni V, et al. MARCKS is a downstream effector in platelet-derived growth factor-induced cell motility in activated human hepatic stellate cells. *Exp Cell Res* 2008;314:1444-54.
- [28] Carloni V, Romanelli RG, Mercurio AM, Pinzani M, Laffi G, Cotrozzi G, et al. Knockout of alpha6 beta1-integrin expression reverses the transformed phenotype of hepatocarcinoma cells. *Gastroenterology* 1998;115:433-42.
- [29] Raggi C, Correnti M, Sica A, Andersen JB, Cardinale V, Alvaro D, et al. Cholangiocarcinoma stem-like subset shapes tumor-initiating niche by educating associated macrophages. *J Hepatol* 2017;66:102-15.
- [30] Chen Q, Jin M, Yang F, Zhu J, Xiao Q, Zhang L. Matrix metalloproteinases: inflammatory regulators of cell behaviors in vascular formation and remodeling. *Mediators Inflamm* 2013;2013:928315.
- [31] Hattermann K, Holzenburg E, Hans F, Lucius R, Held-Feindt J, Mentlein R. Effects of the chemokine CXCL12 and combined internalization of its receptors CXCR4 and CXCR7 in human MCF-7 breast cancer cells. *Cell Tissue Res* 2014;357:253-66.
- [32] Hao M, Zheng J, Hou K, Wang J, Chen X, Lu X, et al. Role of chemokine receptor CXCR7 in bladder cancer progression. *Biochem Pharmacol* 2012;84:204-14.
- [33] Hattermann K, Held-Feindt J, Lucius R, Muerkoster SS, Penfold ME, Schall TJ, et al. The chemokine receptor CXCR7 is highly expressed in human glioma cells and mediates antiapoptotic effects. *Cancer Res* 2010;70:3299-308.
- [34] Chen Y, Teng F, Wang G, Nie Z. Overexpression of CXCR7 induces angiogenic capacity of human hepatocellular carcinoma cells via the AKT signaling pathway. *Oncol Rep* 2016;36:2275-81.
- [35] Lin L, Han MM, Wang F, Xu LL, Yu HX, Yang PY. CXCR7 stimulates MAPK signaling to regulate hepatocellular carcinoma progression. *Cell Death Dis* 2014;5:e1488.

- [36] Neve Polimeno M, Ierano C, D'Alterio C, Simona Losito N, Napolitano M, Portella L, et al. CXCR4 expression affects overall survival of HCC patients whereas CXCR7 expression does not. *Cell Mol Immunol* 2015;12:474-82.
- [37] Nerviani A, Pitzalis C. Role of chemokines in ectopic lymphoid structures formation in autoimmunity and cancer. *J Leukoc Biol* 2018.
- [38] Xin Q, Zhang N, Yu HB, Zhang Q, Cui YF, Zhang CS, et al. CXCR7/CXCL12 axis is involved in lymph node and liver metastasis of gastric carcinoma. *World J Gastroenterol* 2017;23:3053-65.
- [39] Ma DM, Luo DX, Zhang J. SDF-1/CXCR7 axis regulates the proliferation, invasion, adhesion, and angiogenesis of gastric cancer cells. *World J Surg Oncol* 2016;14:256.
- [40] Zhao R, Chang Y, Liu Z, Liu Y, Guo S, Yu J, et al. Effect of vascular endothelial growth factor-C expression on lymph node metastasis in human cholangiocarcinoma. *Oncol Lett* 2015;10:1011-5.
- [41] Barbieri F, Bajetto A, Thellung S, Wurth R, Florio T. Drug design strategies focusing on the CXCR4/CXCR7/CXCL12 pathway in leukemia and lymphoma. *Expert Opin Drug Discov* 2016;11:1093-109.
- [42] Rajagopal S, Kim J, Ahn S, Craig S, Lam CM, Gerard NP, et al. Beta-arrestin- but not G protein-mediated signaling by the "decoy" receptor CXCR7. *Proc Natl Acad Sci U S A* 2010;107:628-32.
- [43] Decaillot FM, Kazmi MA, Lin Y, Ray-Saha S, Sakmar TP, Sachdev P. CXCR7/CXCR4 heterodimer constitutively recruits beta-arrestin to enhance cell migration. *J Biol Chem* 2011;286:32188-97.
- [44] Coggins NL, Trakimas D, Chang SL, Ehrlich A, Ray P, Luker KE, et al. CXCR7 controls competition for recruitment of beta-arrestin 2 in cells expressing both CXCR4 and CXCR7. *PLoS One* 2014;9:e98328.
- [45] Kawamoto M, Umebayashi M, Tanaka H, Koya N, Nakagawa S, Kawabe K, et al. Combined Gemcitabine and Metronidazole Is a Promising Therapeutic Strategy for Cancer Stem-like Cholangiocarcinoma. *Anticancer Res* 2018;38:2739-48.

**Table 1. Clinical and histopathological features of human tissue specimens used for evaluation of CXCR7 expression.** Histological tumor scoring was performed by expert pathologists. The proportion of positive cells was classified into four grades (0, < 1%; 1, 1-30%; 2, 31-50%; 3, 51-100%). Staining intensity was arbitrarily graded from 0 to 3 (0, no staining; 1, weak staining; 2, moderate staining; 3, strong staining). After addition of the two grades, a total staining score for each section was obtained.

Case	Gender	Cancer tissue scoring	Grade	TNM	Angioinvasion	Lymphatic metastases
1	F	4+/5+	G2	pT2bNxM1	N	Y
2	M	2+	G2	N/A	N	N
3	F	3+	G2	pT2aN0Mx	Y	N
4	M	4+	G3	pT1N1	N	Y
5	M	4+	G3	N/A	Y	N
6	M	0	G3	pT3N0Mx	N	N
7	M	5+	G2	pT1N0	N	N
8	M	4+	G2	pT2N0	Y	N
9	M	4+/5+	G1	pT1	N	
10	M	4+/5+	G2	pT2N0M1	N	N
11	F	2+	G2	pT2N0	Y	N
12	F	0	G3	N/A	Y	
13	F	4+	G2	pT3Nx	N	N
14	F	4+	G1	pT1	N	N
15	F	4+	G2	pT1N0	N	N
16	F	4+	G3	pT2bN0	Y	N
17	M	4+	G2	N/A	N	N
18	F	2+	G2	pT2aN0Mx	Y	N
19	F	4+	G3	pT1	N	N
20	F	2+	G1	pT1N0	N	N
21	M	4+	G2	pT1N1Mx	N/A	Y

**Highlights**

- CXCR7 was expressed by different CCA cell lines and in human CCA specimens.
- Interfering with CXCR7 activation in iCCA lines and primary cells reduced migration, invasion, survival and CXCL12-induced adhesion to type I collagen.
- Enrichment of tumor stem-like cells by a 3D culture system resulted in increased CXCR7 expression compared to cells grown in monolayers, and genetic knockdown of CXCR7 reduced sphere formation.
- CXCR7 was found to interact with  $\beta$ -arrestin 2, which was necessary to mediate CXCL12-induced migration, but not survival

ACCEPTED MANUSCRIPT

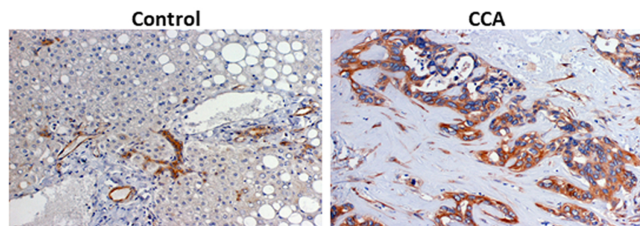
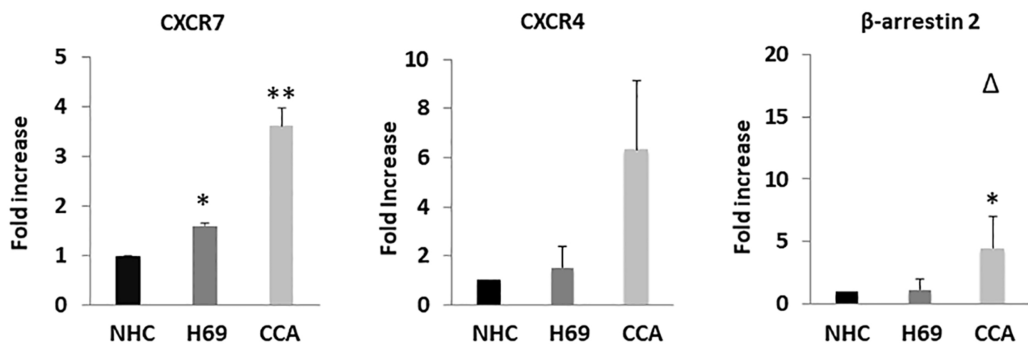
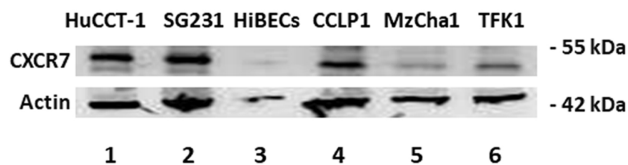
**A****B****C**

Figure 1

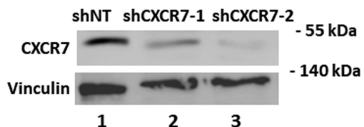
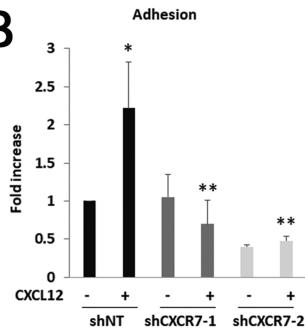
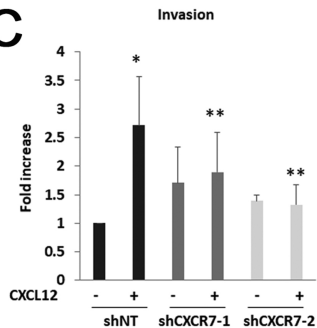
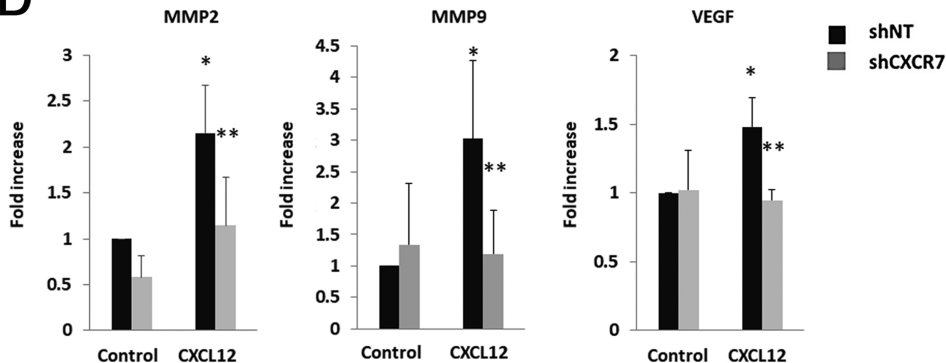
**A****B****C****D**

Figure 2

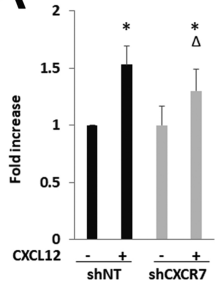
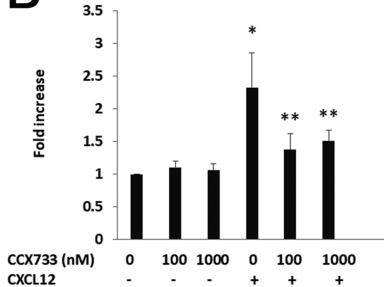
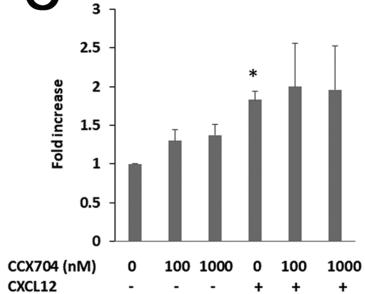
**A****B****C**

Figure 3

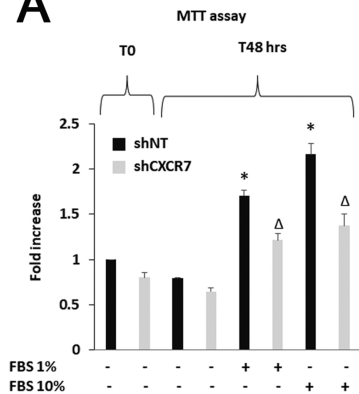
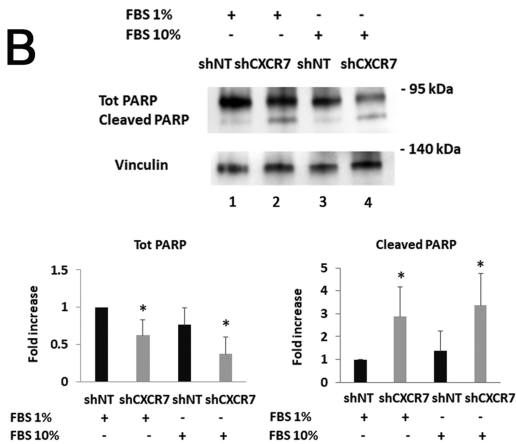
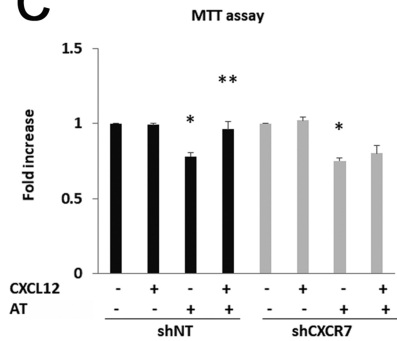
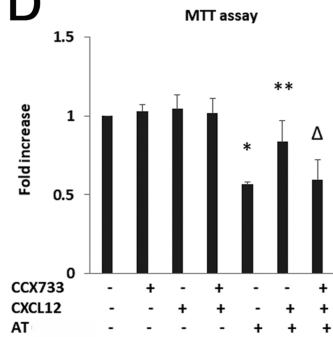
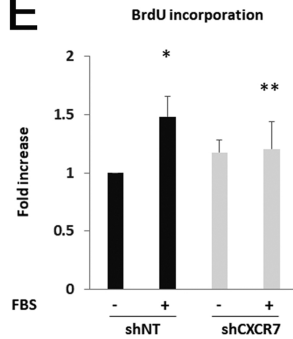
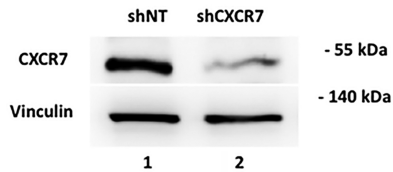
**A****B****C****D****E**

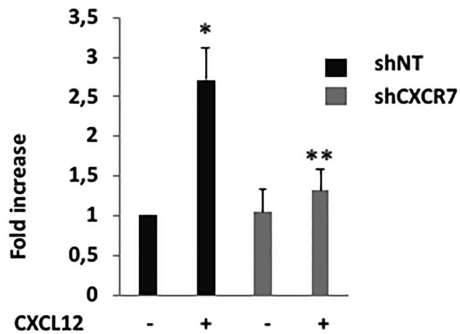
Figure 4

**A**

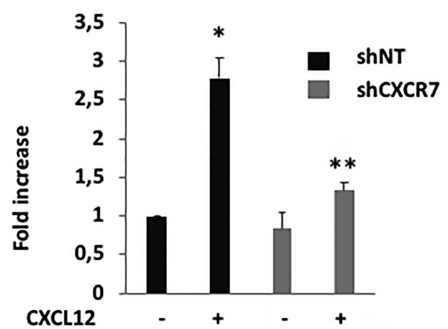
CCLP-1

**B**

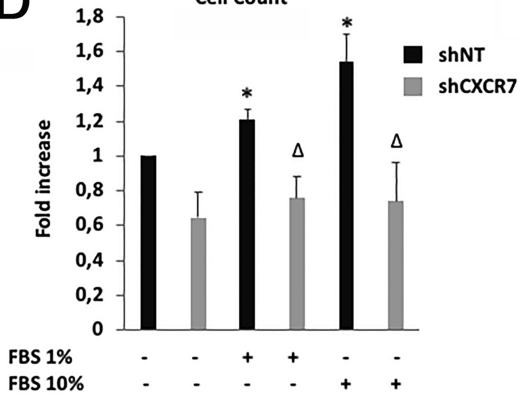
Invasion

**C**

Migration

**D**

Cell Count

**E**

MTT

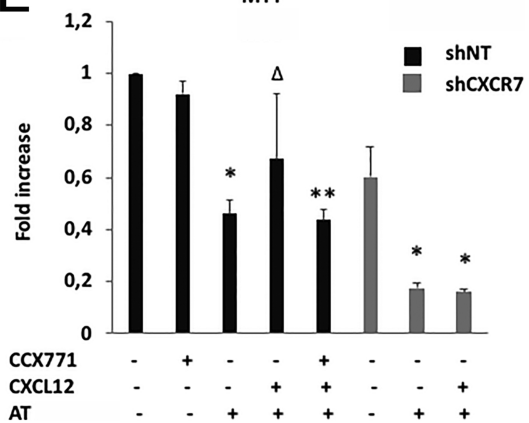


Figure 5

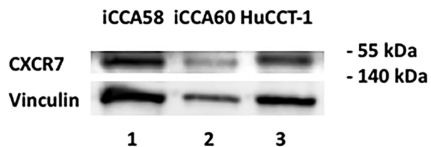
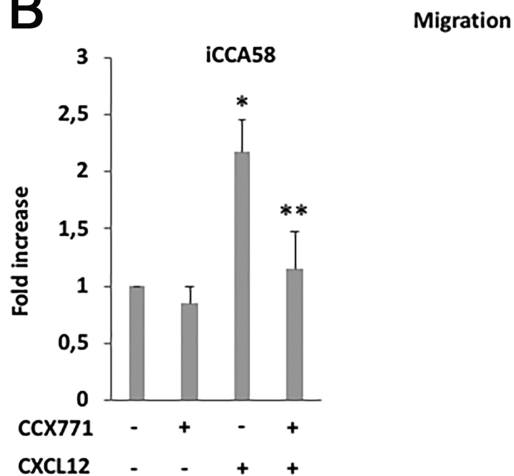
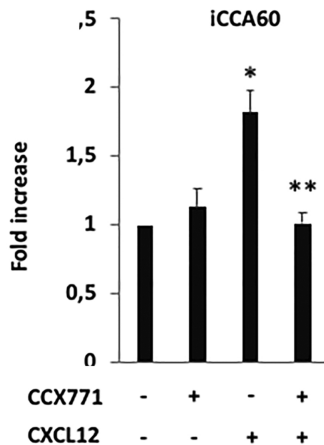
**A****B****C**

Figure 6

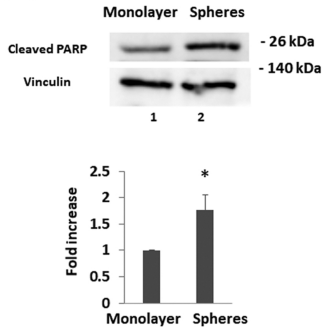
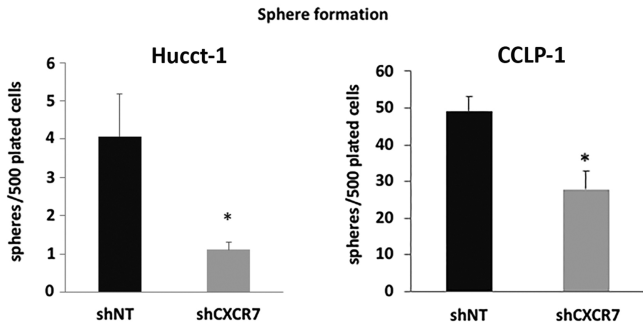
**A****B**

Figure 7

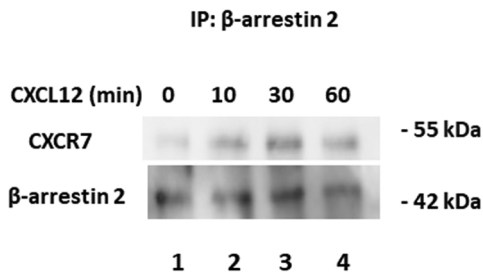
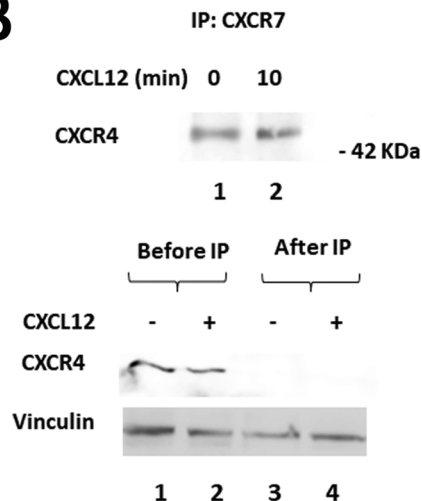
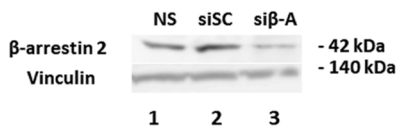
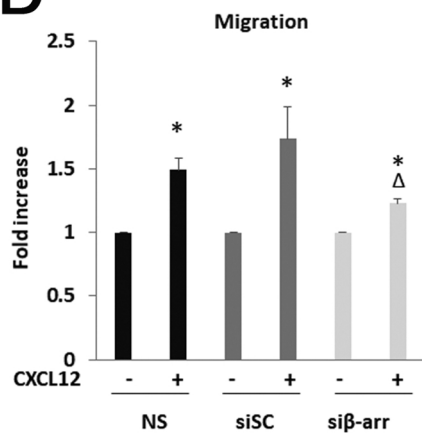
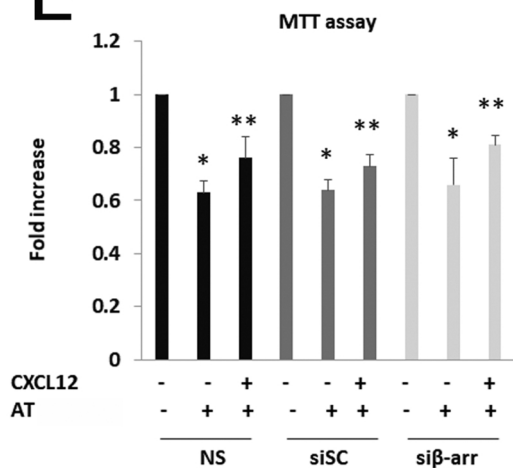
**A****B****C****D****E**

Figure 8

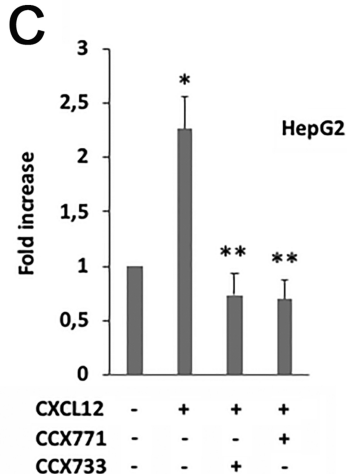
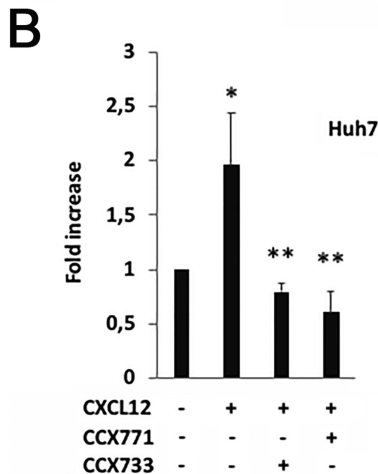
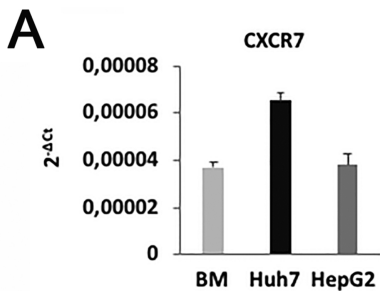


Figure 9